Inorganic Chemistry
Article

Inorg. Chem. **2010**, *49*, 7097–7105 **7097**
DOI: 10.1021/ic100831c

Synthesis and Structural Characterization of a Series of Dimeric Metal(II) Imido Complexes $\{M(\mu\text{-}NAr^{\#})\}_2$ [M = Ge, Sn, Pb; $Ar^{\#} = C_6H_3\text{-}2,6\text{-}(C_6H_2\text{-}2,4,6\text{-}Me_3)_2$] and the Related Monomeric Primary Amido Derivatives $M\{N(H)Ar^{\#}\}_2$ (M = Ge, Sn, Pb): Spectroscopic Manifestations of Secondary Metal−Ligand Interactions

William A. Merrill, Robert J. Wright, Corneliu S. Stanciu, Marilyn M. Olmstead, James C. Fettinger, and Philip P. Power*

Department of Chemistry, One Shields Avenue, University of California, Davis, California 95616

Received May 3, 2010

The solvent-free reaction of $M\{N(SiMe_3)_2\}_2$ (M = Ge, Sn, or Pb) with the sterically encumbered primary amine 2,6-dimesitylaniline $Ar^{\#}NH_2$ [$Ar^{\#} = C_6H_3\text{-}2,6(C_6H_2\text{-}2,4,6\text{-}Me_3)_2$] at ca. 165−175 °C afforded the highly colored imido dimers $\{M(\mu\text{-}NAr^{\#})\}_2$, where M = Ge (**1**), Sn (**2**), or Pb (**3**), with disilylamine elimination. The compounds were characterized by single-crystal X-ray crystallography and heteronuclear NMR spectroscopy. The structures of **1**−**3** were very similar and had nonplanar four-membered M_2N_2 ring cores that are folded along the M—M axis. The nitrogen atoms are planar-coordinated, and the M−N distances are consistent with single bonding. The reaction of $M\{N(SiMe_3)_2\}_2$ with $Ar^{\#}NH_2$ in a 2:1 ratio in solution at lower temperature afforded the relatively stable monomeric primary amido species $M\{N(H)Ar^{\#}\}_2$, where M = Ge (**4**), Sn (**5**), or Pb (**6**). Complexes **4**−**6** displayed V-shaped MN_2 structures, and **5** and **6** revealed close approaches between the metal atom and *ipso*-carbon atoms of two flanking Mes groups of the terphenyl substituents [Sn^{II}—C (2.957 Å) and Pb^{II}—C (2.965 Å)]. The secondary metal−ligand interactions exerted large effects on their electronic and NMR spectra.

Introduction

The heavier group 14 elements Ge, Sn, and Pb form numerous oligomeric metal(II) imides of the formula $(MNR)_n$ (M = Ge, Sn, Pb; R = organic or silyl group; n generally = 4) that often display distorted cubane structures.[1−4] This behavior is in contrast to the congeneric carbon species (organic isocyanides), which generally remain in the form of $R-\overset{+}{N}\equiv\overset{-}{C}:$ monomers and do not readily associate because of efficient hybridization, which promotes strong C−N multiple bonding. Stable heavier group 14 element analogues of isonitriles are currently unknown because the larger size of these elements, combined with weaker π bonds, readily permits association into σ-bonded oligomers, as shown in Scheme 1, for the dimerization "2RNGe" → $\{Ge(NR)\}_2$. The most common heavier group 14 element imido structures are the tetrameric species $\{M(\mu_3\text{-}NR)\}_4$ (M = Ge, Sn, or Pb; R = organic or silyl group), which feature a heterocubane M_4N_4 arrangement of group 14 element and nitrogen atoms (Scheme 2).[1−9]

Scheme 1. Depiction of Two Organoimidogermanium Fragments Undergoing Association To Form a Dimer

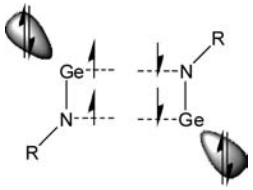

There also exist heterocubane cores of the formula LiM_3N_4[10], fused double-cubane species of the formula $Sn_7(NR)_8$[11] as well as the chalcogenide derivative $M_4N_4E_n$ (E = S or Se; n = 1, 2, or 3).[10,12] Very few lower aggregated species, which possess the potential for multiple bonding between the group 14 element p orbital and nitrogen lone pairs, are known. Rare examples, which are confined to germanium derivatives,[13−15] include the dimeric $\{Ge(\mu\text{-}NR)\}_2$

*To whom correspondence should be addressed. E-mail: pppower@ucdavis.edu.

(1) Veith, M. *Coord. Chem. Rev.* **1990**, *90*, 1.
(2) Veith, M. *Angew. Chem., Int. Ed. Engl.* **1987**, *27*.
(3) Beswick, M. A.; Wright, D. S. *Coord. Chem. Rev.* **1998**, *176*, 373.
(4) Lappert, M. F.; Power, P. P.; Protchenko, A.; Seeber, A. *Metal Amide Chemistry*; Wiley: Chichester, U.K., 2009; Chapter 9.
(5) Veith, M.; Sommer, M.-L.; Jäger, D. *Chem. Ber.* **1979**, *112*, 2581.
(6) Veith, M.; Rechtenwald, O. *Z. Naturforsch.* **1983**, *B38*, 1054.
(7) Chen, H.; Bartlett, R. A.; Dias, H. V. R.; Olmstead, M. M.; Power, P. P. *Inorg. Chem.* **1991**, *30*, 3390.
(8) Allan, R. E.; Beswick, M. A.; Edwards, A. J.; Paver, M. A.; Rennie, M.-A.; Raithby, P. R.; Wright, D. S. *J. Chem. Soc., Dalton Trans.* **1995**, 1991.
(9) Grigsby, W. J.; Hascall, T.; Ellison, J. J.; Olmstead, M. M.; Power, P. P. *Inorg. Chem.* **1996**, *35*, 3254.

Published on Web 07/02/2010

Scheme 2. Aggregation of Heavier Group 14 Element Imides[1−15]

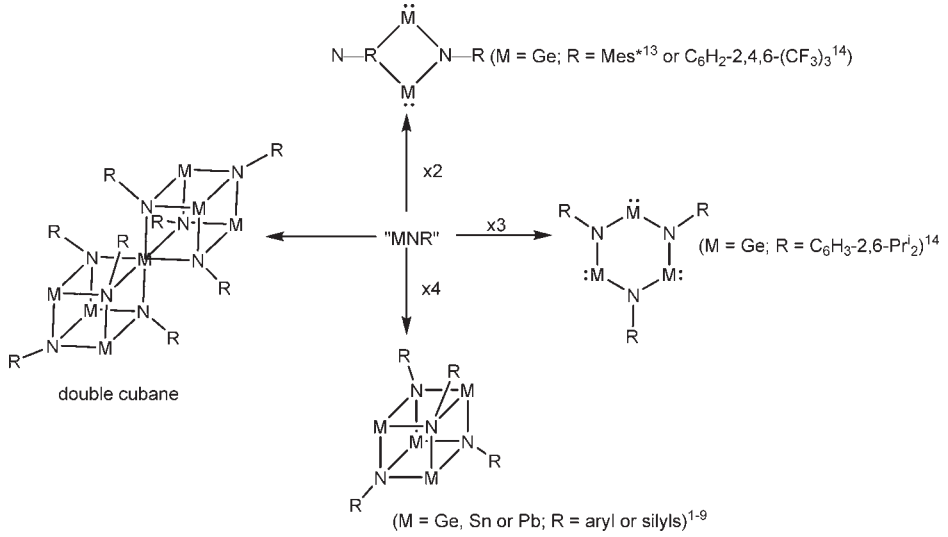

[R = Mes* = C_6H_2-2,4,6-Bu^t_3[13] or R = C_6H_2-2,4,6-$(CF_3)_3$[15]] and the trimeric $\{Ge(\mu\text{-}NC_6H_3\text{-}2,6\text{-}Pr^i_2)\}_3$.[14] Lower aggregates are unknown for either tin or lead. The larger sizes of these elements[16] require exceptionally large substituents to stabilize low coordination and the lower degree of aggregation. Herein we report the reaction of the bulky amine $Ar^{\#}NH_2$ [$Ar^{\#}$ = C_6H_3-2,6-(C_6H_2-2,4,6-Me_3)$_2$][17] with $M\{N(SiMe_3)_2\}_2$ (M = Ge,[18,19] Sn,[18−20] or Pb[18,19]) at elevated temperature. The resulting dimeric imido species are essentially isostructural and possess nonplanar M_2N_2 core arrangements that are bent along their M---M axes and feature dihedral angles of ca. 173° for the germanium derivative (**1**) and ca. 149° for both the tin (**2**) and lead (**3**) derivatives. In addition, we show that the $Ar^{\#}$ group is sufficiently large to stabilize rare examples of monomeric bis(primary amido) $M\{N(H)Ar^{\#}\}_2$ species, which are precedented only by the compounds $Ge\{N(H)Mes^*\}_2$[13] and $Sn\{N(H)Mes^*\}_2$.[21]

Experimental Section

General Procedures. All manipulations were performed with the use of modified Schlenk techniques under N_2 or in a Vacuum Atmospheres drybox under N_2. Solvents were distilled over Na/K and degassed immediately prior to use via freeze−pump−thaw cycles. Unless otherwise noted, all chemicals were obtained from commercial sources and used without further purification. $Ar^{\#}NH_2$[8] and $M\{N(SiMe_3)_2\}_2$ (M = Ge, Sn, or Pb)[19] were prepared according to literature procedures.

All physical measurements were performed under strictly anaerobic and anhydrous conditions. ^1H and ^{13}C NMR spectra were acquired on a Varian Mercury 300 MHz instrument and referenced internally to either residual protio benzene or trace silicone vacuum grease (δ 0.29 ppm in C_6D_6). ^{119}Sn NMR spectra were acquired a Bruker 500 MHz (186 MHz) instrument and were referenced externally to $SnBu^n_4$ in C_6D_6 (δ −11.7 ppm).[22] ^{207}Pb NMR spectra were recorded on a Bruker 500 MHz instrument (ca. 105 MHz) and were externally referenced to $Pb(NO_3)_2$ in D_2O (δ −2984.4 ppm).[23] IR spectra were recorded as Nujol mulls between CsI plates on a Perkin-Elmer 1430 spectrophotometer. UV−visible spectra were recorded as dilute hexane solutions in 3.5 mL quartz cuvettes using a HP 8452 diode-array spectrophotometer.[12] Melting points were determined on a Meltemp II apparatus using glass capillaries sealed with vacuum grease and are uncorrected.

X-ray Crystallography. Crystals of appropriate quality for X-ray diffraction studies were removed from a Schlenk tube under a stream of nitrogen and immediately covered with a thin layer of hydrocarbon oil (Paratone-N). A suitable crystal was selected, attached to a glass fiber, and quickly placed in a low-temperature stream of nitrogen [90(2) K].[22] Data for all compounds were obtained on a Bruker SMART 1000 or SMART APEX instrument using Mo Kα radiation (λ = 0.710 73 Å) in conjunction with a CCD detector. The collected reflections were corrected for Lorentz and polarization effects by using Blessing's method as incorporated into the program *SADABS*.[24,25] The structures were solved by direct methods and refined with the *SHELXTL*, version 6.1, software package.[26] Refinement was by full-matrix least-squares procedures, with all carbon-bound hydrogen atoms included in calculated positions and treated as riding atoms. Nitrogen-bound hydrogen atoms were located in different Fourier maps and refined with N−H distance restraints of 0.90(2) Å in **4**−**6**. A summary of the crystallographic and data collection parameters for **1**−**6** is given in Table 1.

(10) Chivers, T.; Eisler, D. J. *Angew. Chem., Int. Ed.* **2004**, *43*, 6686.
(11) Armstrong, D. R.; Benevelli, F.; Bond, A. D.; Feeder, N.; Harron, E. A.; Hopkins, A. D.; McPartlin, M.; Moncrieff, D.; Sáez, D.; Quadrelli, E. A.; Woods, A. D.; Wright, D. A. *Inorg. Chem.* **2002**, *41*, 1492.
(12) Chivers, T.; Clark, T. J.; Krahn, M.; Parvez, M.; Schatte, G. *Eur. J. Inorg. Chem.* **2003**, 1857.
(13) Hitchcock, P. B.; Lappert, M. F.; Thorne, A. J. *J. Chem. Soc., Chem. Commun.* **1990**, 1587.
(14) Bartlett, R. A.; Power, P. P. *J. Am. Chem. Soc.* **1990**, *112*, 3660.
(15) Ahlemann, J.-T.; Roesky, H. W.; Murugavel, R.; Parisini, E.; Noltemeyer, M.; Schmidt, H.-G.; Muller, O.; Herbst-Irmer, R.; Markovskii, L. N.; Shermolovich, Y. G. *Chem. Ber.* **1997**, *130*, 1113.
(16) Pyykkö, P.; Matsumi, S. *Chem.—Eur. J.* **2009**, *15*, 186.
(17) Tilley, T. D.; Gavenonis, J. *Organometallics* **2000**, *21*, 5549.
(18) Harris, D. H.; Lappert, M. F. *J. Chem. Soc., Chem. Commun.* **1974**, 895.
(19) Gynane, M. J. S.; Harris, D. H.; Lappert, M. F.; Power, P. P.; Rivière, P.; Rivière-Baudet, M. *J. Chem. Soc., Dalton Trans.* **1977**, 2004.
(20) Schaeffer, C. D.; Zuckerman, J. J. *J. Am. Chem. Soc.* **1974**, *98*, 7160.
(21) Çetinkaya, B.; Hitchcock, P. B.; Lappert, M. F.; Misra, M. C.; Thorne, A. J. *J. Chem. Soc., Chem. Commun.* **1984**, 148.
(22) Wrackmeyer, B.; Horchler, K. *Annu. Rep. NMR Spectrosc.* **1989**, *22*, 249.
(23) Wrackmeyer, B.; Horchler, K.; Zhou, K.; Veith, M. *Z. Naturforsch.* **1989**, *44b*, 288.
(24) Hope, H. *Prog. Inorg. Chem.* **1995**, *41*, 1.
(25) (a) Blessing, R. H. *Acta Crystallogr.* **1995**, *A51*, 33–38. (b) Sheldrick, G. M. *SADABS* Siemens Area Detector Absorption Correction; Universität Göttingen: Göttingen, Germany, 2008.
(26) (a) Sheldrick, G. M. *Acta Crystallogr.* **2008**, *A64*, 112.

Table 1. Selected Crystallographic Data for Imido Compounds **1**−**3**

compound	{Ge(μ-NAr#)}$_2$ (**1**)	{Sn(μ-NAr#)}$_2$ (**2**)	{Pb(μ-NAr#)}$_2$ (**3**)
formula	$Ge_2N_2C_{24}H_{25}$	$Sn_2N_2C_{24}H_{25}$	$Pb_2N_2C_{24}H_{25}$
fw	800.08	892.28	1069.28
color, habit	red-orange, block	red, rod	dark violet, block
cryst syst	triclinic	monoclinic	monoclinic
space group	$P\bar{1}$	$P2_1/n$	$P2_1/n$
a, Å	11.1086(12)	12.6268(11)	12.6502(5)
b, Å	11.9616(13)	21.1020(19)	21.1889(8)
c, Å	15.657(2)	16.2797(14)	16.3957(6)
α, deg	93.649(2)	90	90
β, deg	91.118(2)	111.470(3)	112.2590(10)
γ, deg	95.606(2)	90	90
V, Å^3	2065.6(4)	4036.7(6)	4067.3(3)
Z	2	4	4
cryst dimens, mm	0.45 × 0.38 × 0.26	0.07 × 0.04 × 0.02	0.28 × 0.32 × 0.19
T, K	90(2)	90(2)	90(2)
d_{calc}, g/cm^3	1.286	1.277	1.746
abs coeff *μ*, mm^{-1}	1.489	1.273	8.303
θ range, deg	1.30−27.48	1.65−27.48	1.65−27.54
R(int)	0.0176	0.0605	0.0388
obsdreflns [$I > 2\sigma(I)$]	8202	6355	8014
data/restraints/param	9471/0/481	9240/0/481	9371/0/481
R1, obsd reflns	0.0323	0.0449	0.0202
wR2, all	0.0920	0.1177	0.0501

compound	Ge{N(H)Ar#}$_2$ (**4**)	Sn{N(H)Ar#}$_2$ (**5**)	Pb{N(H)Ar#}$_2$ (**6**)
formula	$GeN_2C_{48}H_{52}$	$SnN_2C_{48}H_{52}$	$PbN_2C_{48}H_{52}$
fw	729.51	775.61	864.11
color, habit	yellow, parallelepiped	orange, plate	yellow, plate
cryst syst	monoclinic	triclinic	triclinic
space group	*C*2/*c*	$P\bar{1}$	$P\bar{1}$
a, Å	19.0482(8)	9.7754(9)	9.7905(6)
b, Å	15.1138(6)	11.7530(11)	11.8159(8)
c, Å	16.7892(7)	18.0055(17)	17.9985(12)
α, deg	90	73.768(2)	72.9850(10)
β, deg	123.3110(10)	87.967(2)	88.1780(10)
γ, deg	90	88.886(2)	89.0400(10)
V, Å^3	4039.3(3)	1984.8(3)	1973.5(2)
Z	4	2	2
cryst dimens, mm	0.36 × 0.26 × 0.16	0.47 × 0.36 × 0.17	0.41 × 0.35 × 0.17
T, K	90(2)	90(2)	90(2)
d_{calc}, g/cm^3	1.200	1.298	1.454
abs coeff *μ*, mm^{-1}	0.793	0.679	4.310
θ range, deg	1.86−30.00	1.80−30.00	1.18−27.50
R(int)	0.0314	0.0212	0.0232
obsd reflns [$I > 2\sigma(I)$]	4927	9621	8115
data/restraints/param	5889/2/252	11448/2/489	9054/2/480
R1, obsd reflns	0.0350	0.0358	0.0227
wR2, all	0.0975	0.1017	0.0568

{Ge(μ-NAr#)}$_2$ (1). Ar#NH$_2$ (0.329 g, 1 mmol) and Ge(N(SiMe$_3$)$_2$)$_2$ (0.433 g, 1.1 mmol) were combined in a Schlenk flask and heated at 165 °C in an oil bath for ca. 10 min with stirring. A red melt resulted, and the evolution of vapor was observed. Heating was continued over ca. 5 min, and reduced pressure was applied to afford an orange-red solid. The volatile HN(SiMe$_3$)$_2$ byproduct and any excess Ge{N(SiMe$_3$)$_2$}$_2$ were removed by distillation. The residue was extracted with ca. 20 mL hexanes and filtered over a Celite-padded frit. The filtrate was concentrated under reduced pressure to ca. 10 mL, and storage at 7 °C afforded X-ray-quality crystals of **1** as orange-red blocks. Yield: 0.108 g, 14% based on Ge. Mp: 285 °C. UV−vis [*λ*, nm (*ε*, M^{-1} cm^{-1})]: 322 (9500), 356 sh (6300), 388 sh (4100), 490 (400). IR (cm^{-1}): *ν*(N−Ge) 440, 347, 328. ^{1}H NMR (300 MHz, 25 °C, C$_6$D$_6$): *δ* 1.99 (s, 24H, Mes *o*-C*H*$_3$), 2.23 (s, 12H, Mes *p*-C*H*$_3$), 6.81 (t, 2H, *p*-H), 6.85 (s, 8H, Mes−*H*), 6.91 (d, 4H, *m*-H). ^{13}C{^{1}H} NMR (75 MHz, C$_6$D$_6$): *δ* 20.19 (*o*-*C*H$_3$), 20.50 (*p*-*C*H$_3$), 119.83, 128.45, 130.97, 136.05, 136.17, 137.85, 145.11 (Ar*C*). ^{73}Ge NMR: no signal observed.

{Sn(μ-NAr#)}$_2$ (2). Ar#NH$_2$ (0.329 g, 1.00 mmol) and Sn{N(SiMe$_3$)$_2$}$_2$ (0.461 g, 1.05 mmol) were combined in a Schlenk flask, and reaction and product workup were performed in a manner similar to that described for **1**. This afforded the product **2** as deep-red rod-shaped crystals. Yield: 0.350 g, 38% based on Sn. Mp: 235−240 °C. UV−vis [*λ*, nm (*ε*, M^{-1} cm^{-1})]: 348 (8400), 410 (7800), 456 sh (4800). IR (cm^{-1}): *ν*(N−Sn) 410, 385, 335, 305. ^{1}H NMR (300 MHz, 25 °C, C$_6$D$_6$): *δ* 2.07 (s, 24H, Mes *o*-C*H*$_3$), 2.22 (s, 12H, Mes *p*-C*H*$_3$), 6.67 (t, 2H, *p*-H), 6.84 (s, 8H, Mes−H), 6.96 (d, 4H, *m*-H). ^{13}C{^{1}H} NMR (75 MHz, 25 °C, C$_6$D$_6$): *δ* 20.92 (*o*-CH$_3$), 21.80 (*p*-CH$_3$), 117.95, 129.39, 129.61, 131.09, 136.97, 137.05 (ArC). ^{119}Sn{^{1}H} NMR (186.49 MHz, C$_6$D$_6$): *δ* 738.9.

{Pb(μ-NAr#)}$_2$ (3). In a manner similar to that described for **1**, Ar#NH$_2$ (0.165 g, 0.50 mmol) and Pb(N(SiMe$_3$)$_2$)$_2$ (0.290 g, 0.55 mmol) were combined in a Schlenk flask and heated to 175 °C in an oil bath with stirring to afford the crude product **3** as a dark-violet solid. Further heating and workup similar to that described for **1** afforded crystalline **3** as dark-violet blocks of sufficient quality for X-ray diffraction studies. Yield: 0.100 g (17% based on Pb). Mp: 261 °C. UV−vis [*λ*, nm (*ε*, M^{-1} cm^{-1})]: 352 (8400), 490 (14 700). IR (cm^{-1}): *ν*(N−Pb) 460, 390. ^{1}H NMR (300 MHz, 25 °C, C$_6$D$_6$): *δ* 2.12 (s, 24H, Mes *o*-C*H*$_3$), 2.18 (s, 12H, Mes *p*-C*H*$_3$), 6.38 (t, 2H, *p*-H), 6.77 (s, 8H, Mes−*H*), 6.89 (d, 4H, *m*-H). ^{13}C{^{1}H} NMR (75 MHz, C$_6$D$_6$): *δ* 21.34 (*o*-*C*H$_3$), 22.06 (*p*-*C*H$_3$), 118.03, 119.46, 129.72, 130.65, 130.86, 137.90, 138.90, 139.82 (Ar*C*). ^{207}Pb{^{1}H} NMR (105.15 MHz, C$_6$D$_6$): *δ* 5019.

Ge{N(H)Ar$^{\#}$}$_2$ (4). To Ar$^{\#}$NH$_2$ (0.861 g, 2 mmol) in toluene (20 mL) was added dropwise Ge{N(SiMe$_3$)$_2$}$_2$ (0.393 g, 1 mmol) in toluene (15 mL) at ca. 0 °C. The mixture was stirred and allowed to warm to room temperature over the next 12 h to afford a pale-yellow solution, which was filtered over a Celite-padded frit. Concentration of the filtrate under reduced pressure to about half the original volume and storage at −13 °C afforded yellow diamond-shaped X-ray-quality crystals of **4**. Yield: 0.153 g, 21% based on Ge. Mp: 198 °C (turns orange). UV−vis [λ, nm (ε, M^{-1} cm^{-1})]: 380 (13 700). IR (cm^{-1}): ν(Ar$^{\#}$N−(H)$_2$) 3480, ν(GeN−H) 3380, 3350, 3320, ν(N−Ge) 450, 395, 280. ^{1}H NMR (300 MHz, 25 °C, C$_6$D$_6$): δ 1.91 (s, 24H, Mes *o*-C*H*$_3$), 2.21 (s, 12H, Mes *p*-C*H*$_3$), 2.98 (s, Ar$^{\#}$N*H*$_2$), 5.46 (s, 2H, Ar$^{\#}$N*H*−Ge), 6.75 (t, 2H, *p*-H), 6.77 (s, 8H, Mes−*H*), 6.84 (d, 4H, *m*-H). ^{13}C{^{1}H} NMR (75 MHz, 25 °C, C$_6$D$_6$): δ 19.91 (*o*-*C*H$_3$), 21.19 (*p*-*C*H$_3$), 119.22, 128.81, 129.16, 130.97, 136.69, 136.91, 144.17 (Ar*C*).

Sn{N(H)Ar$^{\#}$}$_2$ (5). To Ar$^{\#}$NH$_2$ (0.861 g, 2 mmol) in toluene (20 mL) was added dropwise Sn{N(SiMe$_3$)$_2$}$_2$ (0.439 g, 1 mmol) in 15 mL of toluene at ca. 0 °C. Reaction conditions and product workup similar to those described for **4** afforded orange plates of **5** that were suitable for X-ray diffraction studies. Yield: 0.295 g, 38% based on Sn. Mp: 241 °C (turns red). UV−vis [λ, nm (ε, M^{-1} cm^{-1})]: 420 (5000). IR (cm^{-1}): ν(Ar$^{\#}$N−(H)$_2$) 3480, ν(**5** N−H) 3380, 3325, ν(N−Sn) 445, 425, 390, 280. ^{1}H NMR (300 MHz, 25 °C, C$_6$D$_6$): δ 2.01 (s, 24H, Mes *o*-C*H*$_3$), 2.19 (s, 12H, Mes *p*-C*H*$_3$), 2.98 (s, Ar$^{\#}$N*H*$_2$), 4.88 (s, 2H, Ar$^{\#}$N*H*−Sn), 6.73 (t, 2H, *p*-H), 6.82 (s, 8H, Mes−*H*), 6.88 (d, 4H, *m*-H). ^{13}C{^{1}H} NMR (75 MHz, 25 °C, C$_6$D$_6$): δ 20.03 (*o*-*C*H$_3$), 21.08 (*p*-*C*H$_3$), 116.86, 127.16, 128.66, 129.61, 137.19 (Ar*C*). ^{119}Sn-{^{1}H} NMR (186.49 MHz, 25 °C, C$_6$D$_6$): δ 118.9.

Pb{N(H)Ar$^{\#}$}$_2$ (6). To Ar$^{\#}$NH$_2$ (0.861 g, 2 mmol) in toluene (20 mL) was added Pb{N(SiMe$_3$)$_2$}$_2$ (0.528 g, 1 mmol) in 40 mL of toluene at ca. 0 °C. Reaction conditions and product workup similar to those described for **4** afforded yellow-orange plates of **6** that were suitable for X-ray diffraction studies. Yield: 0.100 g, 11% based on Pb. Mp: 205 °C (dec, turns deep red). UV−vis [λ, nm (ε, M^{-1} cm^{-1})]: 448 (3800). IR (cm^{-1}): ν(Ar$^{\#}$N−(H)$_2$) 3480, ν(N−H) 3430, 3390, 3350, ν(N−Pb) 395. ^{1}H NMR (300 MHz, 25 °C, C$_6$D$_6$): δ 2.05 (s, 24H, Mes *o*-C*H*$_3$), 2.16 (s, 12H, Mes *p*-C*H*$_3$), 2.98 (s, Ar$^{\#}$N*H*$_2$), 5.74 (s, 2H, Ar$^{\#}$N*H*−Pb), 6.64 (t, 2H, *p*-H), 6.81 (s, 8H, Mes−*H*), 6.92 (d, 4H, *m*-H). ^{13}C{^{1}H} NMR (75 MHz, 25 °C, C$_6$D$_6$): δ 20.75 (*o*-*C*H$_3$), 21.77 (*p*-*C*H$_3$), 115.75, 118.50, 129.20, 130.35,137.76, 138.05, 138.90, 152.55 (Ar*C*). ^{207}Pb{^{1}H} NMR (104.92 MHz, 25 °C, C$_6$D$_6$): δ 2871.

Results and Discussion

Synthesis. At room temperature, it was observed that both Sn{N(SiMe$_3$)$_2$}$_2$ and Pb{N(SiMe$_3$)$_2$}$_2$ cause rapid surface darkening of crystalline H$_2$NAr$^{\#}$ (the color resembled those later observed for the imidotin and -lead derivatives **2** and **3**) when the two solids were placed together in a Schlenk flask. As a result, it was decided to prepare **1**−**3** without a solvent by the reaction of M{N(SiMe$_3$)$_2$}$_2$ (M = Ge, Sn, or Pb) with 2,6-dimesitylaniline H$_2$NAr$^{\#}$, according to eq 1, while removing the HN(SiMe$_3$)$_2$ byproduct under reduced pressure. The products could be readily purified by crystallization from hexane. They were isolated as orange-red (**1**), dark-red (**2**), or dark-purple (**3**) moderately air- and moisture-sensitive crystals.

$$\mathrm{ArNH_2} + \mathrm{M\{N(SiMe_3)_2\}_2} \xrightarrow{165-175\ ^\circ\mathrm{C}} \frac{1}{2}\{\mathrm{M}(\mu\text{-NAr})\}_2 + 2\mathrm{HN(SiMe_3)_2} \quad (1)$$

The bis(primary amide) compounds **4**−**6** were prepared by the 2:1 reaction of H$_2$NAr$^{\#}$ and metal silylamides in a toluene solution. Attempts to synthesize **4**−**6** by an approach similar to that used for **1**−**3** but with a 2:1 H$_2$NAr$^{\#}$/M{N(SiMe$_3$)$_2$}$_2$ ratio of reactants resulted in the formation of the corresponding imido products **1**−**3**. Furthermore, attempts to synthesize **4**−**6** by the more traditional salt metathesis route, i.e., 2LiN(H)Ar$^{\#}$ with GeCl$_2$(1,4-dioxane), SnCl$_2$, or PbBr$_2$ in Et$_2$O, resulted in very low yields of impure products. Thus, the transamination approach was revisited, and it was found that imide formation could be suppressed by the slow addition of a solution of M{N(SiMe$_3$)$_2$}$_2$ to 2 equiv of H$_2$NAr$^{\#}$ in a toluene solution at ca. 0 °C. This afforded crystals of **4**−**6** from concentrated toluene solutions at ca. −13 °C. The temperature-related preference for an imido rather than a bisamido product was further supported by spectroscopic data. ^{1}H NMR spectroscopy of crude reaction mixtures of the bisamides **4**−**6** displayed a signal at δ 2.98, characteristic of H$_2$NAr$^{\#}$. ^{1}H NMR signals attributable to the imido products **1**−**3** were also observed in these reaction mixtures. Furthermore, ^{1}H NMR spectroscopy of solutions of freshly crystallized samples of **4**−**6** revealed the presence of small amounts of free H$_2$NAr$^{\#}$ (see the Experimental Section). The appearance of the ν(N−H) stretching absorption characteristic of the N−H hydrogen atoms of free H$_2$NAr$^{\#}$ at 3480 cm^{-1} in the IR spectra of Nujol mulls of crystalline **4**−**6** also supported the existence of an equilibrium between the bisamido compounds **4**−**6** and the corresponding imido species **1**−**3** and H$_2$NAr$^{\#}$, as shown in eq 2.

$$2\mathrm{M\{N(H)Ar\}_2} \rightarrow \{\mathrm{M}(\mu\text{-NAr})\}_2 + 2\mathrm{H_2NAr} \quad (2)$$

In addition, it was observed that crystalline samples of **4**−**6** all darken to colors resembling those of the imido species **1**−**3**, respectively, upon heating inside the Meltemp II apparatus. The facility of this conversion seems to follow the order Pb (**6**) > Sn (**5**) > Ge (**4**).

^{1}H NMR and IR spectroscopies of crude and "pure" crystalline samples of the bisamides **4**−**6** show clearly that both the imido- and bis(primary amido)metal(II) species are present in solutions of **4**−**6**. The coexistence of amido and imido species was also reported for Ge{N(H)Mes*}$_2$ and {Ge(μ-NMes*)}$_2$.[13] Equations 3−5 illustrate an alternative pathway by which the bisamides **4**−**6** might transform to free H$_2$NAr$^{\#}$ and **1**−**3** and show how this reaction might occur through the putative intermediate "{Ar$^{\#}$(H)-N−M−N(SiMe$_3$)$_2$}$_2$" during the synthetic route to the imides **1**−**3**. The existence of the heteroleptic

$$\mathrm{H_2NAr} + \mathrm{M\{N(SiMe_3)_2\}_2} \leftrightarrows \frac{1}{2}\{\mathrm{Ar(H)N-M-N(SiMe_3)_2\}_2} + \mathrm{HN(SiMe_3)_2} \quad (3)$$

$$\mathrm{\{Ar(H)N-M-N(SiMe_3)_2\}_2} \leftrightarrows \frac{1}{2}(\mathrm{MNAr})_2 + \mathrm{HN(SiMe_3)_2} \quad (4)$$

$$\mathrm{\{Ar(H)N-M-N(SiMe_3)_2\}_2} + \mathrm{H_2NAr} \leftrightarrows \mathrm{M\{N(H)Ar\}_2} + \mathrm{HN(SiMe_3)_2} \quad (5)$$

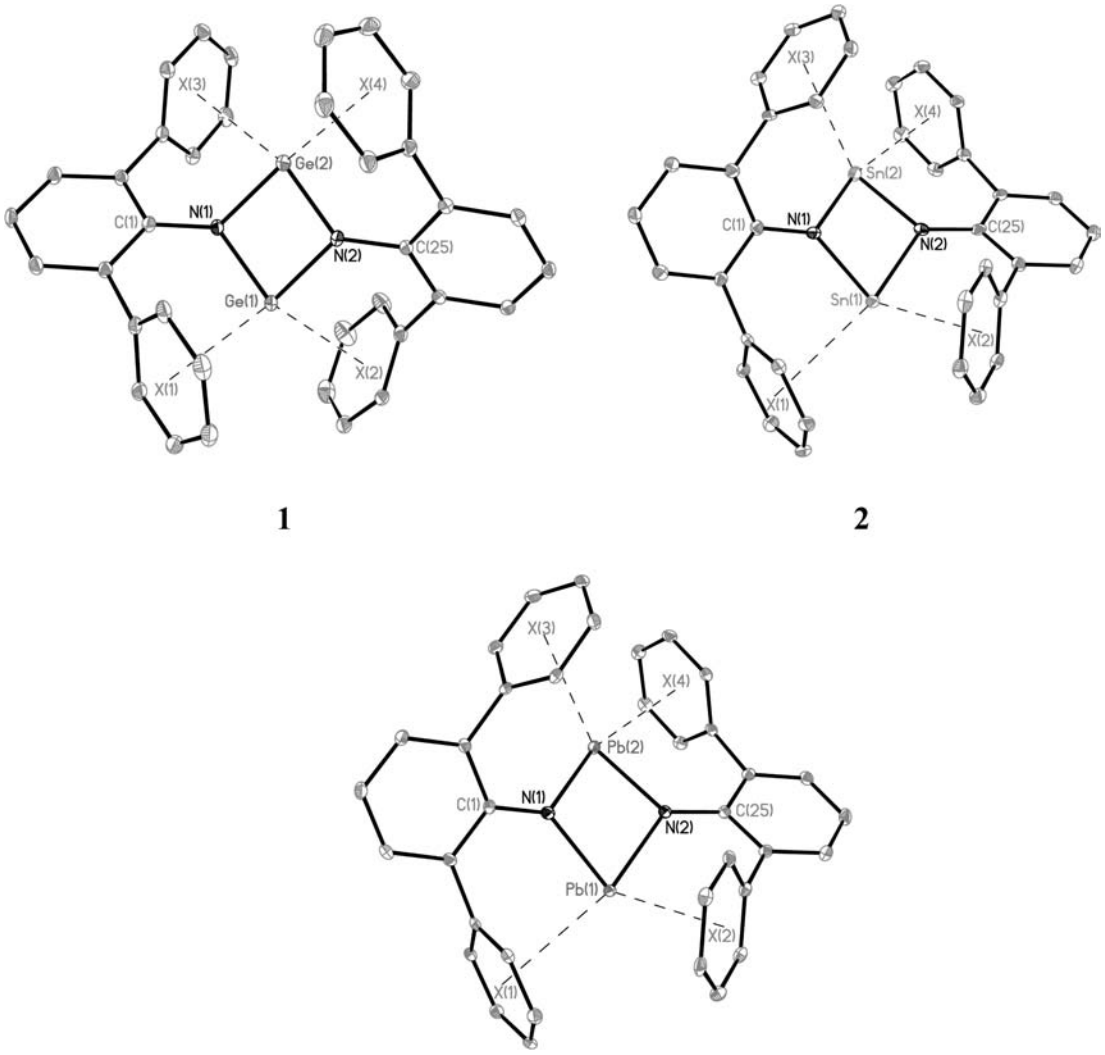

Figure 1. Thermal ellipsoid (30%) drawings of **1**−**3**. Hydrogen atoms and methyl groups are not shown. Ge(1)---Ge(2) 2.860 Å. Ge(1,2)−N(1,2) 1.885 Å (average); metal---centroid interactions range from Ge(1)---X(1) 3.127 Å to Ge(2)---X(3) 3.592 Å. Sn(1)---Sn(2) 3.193 Å. Sn(1,2)−N(1,2) 2.105 Å (average); metal---centroid interactions range from Sn(2)---X(4) 3.159 Å to Sn(1)---X(2) 3.286 Å. Pb(1)---Pb(2) 3.375 Å; N(1,2)−Pb(1,2) 2.211 Å (average); metal---centroid interactions range from Pb(2)---X(4) 3.115 Å to Pb(2)---X(3) 3.262 Å.

$\{Ar(H)N-M-N(SiMe_3)_2\}_2$ in eqs 3−5 is supported by ^{1}H NMR spectroscopy of an orange crystalline product, which was obtained from a solution reaction mixture of $Ge\{N(SiMe_3)_2\}_2$ and $H_2NAr^{\#}$. A ^{1}H NMR spectrum of a C_6D_6 solution of these crystals revealed a large silyl peak (δ −0.020), along with 2:1 (Mes−CH_3) singlets at δ 2.162 and 2.186, chemical shifts that are different from those of **1** or **4**. The integrations of these alkyl and silyl peaks revealed ca. a 1:1 ratio, consistent with the formulation $Ge\{N(H)Ar^{\#}\}N(SiMe_3)_2$. X-ray diffraction studies revealed them to have a heteroleptic amido-bridged dimeric structure that was of insufficient quality for publication.

The tendency for an equilibrium to exist between an −{N(H)R}-bearing heavier group 14 compound and its related imido derivative was also observed in the recently reported amido-bridged dimeric species $Sn_2\{N(H)C_6H_3$-2,6-$Pr^i_2\}_4$, which was shown to convert spontaneously to the known heterocubane $\{Sn(\mu$-NC_6H_3-2,6-$Pr^i_2)\}_4$ and free 2,6-diisopropylaniline under ambient conditions.[27,28] In contrast, the bis(primary amide) compounds **4**−**6** are much more stable than $Sn_2\{N(H)Dipp\}_4$. It seems probable that the association reactions to afford dimeric structures occur prior to amine elimination and are inhibited by the bulkier $Ar^{\#}$ substituent at nitrogen. The inhibition of reactions by the replacement of less bulky organic substituents with terphenyls was also demonstrated earlier by Protasiewicz and co-workers for chlorine-atom-transfer equilibria between aryldichlorophosphines and aryldiphosphenes.[19] This influence of steric hindrance on the reaction rates is also evident from the comparison of the synthesis of the dimer **1** with that of the trimer$\{Ge(\mu$-NC_6H_3-2,6-$Pr^i_2)\}_3$.[7,14] The latter species could be obtained at a much lower reaction temperature (ca. 60 °C) than that required for the dimer (ca. 165 °C), most likely

(27) Merrill, W. A.; Steiner, J.; Betzer, A.; Nowik, I.; Herber, R.; Power, P. P. *Dalton Trans*. **2008**, 5905.

(28) Smith, R. C.; Shah, S.; Urnezius, E.; Protasiewicz, J. D. *J. Am. Chem. Soc*. **2002**, *125*, 40.

Table 2. Selected Interatomic Distances (Å) and Angles (deg) for Compounds **1**−**3**[a]

	{Ge(μ-NAr#)}2 (**1**)	{Sn(μ-NAr#)}2 (**2**)	{Pb(μ-NAr#)}2 (**3**)
M(1)−N(1)	1.8869(15)	2.093(4)	2.199(3)
M(2)−N(1)	1.8795(15)	2.114(4)	2.222(2)
M(1)−N(2)	1.8906(15)	2.113(4)	2.219(2)
M(2)−N(2)	1.8860(15)	2.097(4)	2.204(3)
N(1)−C(1)	1.396(2)	1.390(6)	1.378(4)
N(1)−C(25)	1.394(2)	1.388(6)	1.377(4)
N(1)−M(1)−N(2)	81.01(6)	77.66(15)	76.9(4)
N(1)−M(2)−N(2)	81.32(6)	77.57(14)	76.8(4)
M(1)−N(1)−M(2)	99.10(7)	98.75(16)	98.50(10)
M(1)−N(2)−M(2)	98.39(7)	98.66(16)	99.47(10)
M(1)---X(1)	3.127(2)	3.174(5)	3.168(2)
M(1)---X(2)	3.243(2)	3.286(5)	3.250(4)
M(2)---X(3)	3.592(2)	3.254(5)	3.262(4)
M(2)---X(4)	3.310(2)	3.159(5)	3.115(4)
X(1)---M(1)---X(2)	128.5(2)	99.9(5)	101.9(4)
X(3)---M(2)---X(4)	131.8(2)	104.1(5)	105.5(4)
dihedral N−M(1)−N/X---M(1)---X	56.6(3)	58.5(5)	58.9 (4)
dihedral N−M(2)−N/X---M(2)---X	49.8(3)	51.9(5)	52.9 (4)
fold angle along the M---M axis	172.4	148.3	148.3

[a] X represents the centroid of the flanking aryl ring.

because of the lower steric requirements of 2,6-diisopropylaniline in comparison to $Ar^{\#}NH_2$.

Structures. The structures of **1**−**3** are illustrated in Figure 1. Selected interatomic distances and angles are listed in Table 2. The compounds consist of dimeric units that feature rhomboid M_2N_2 cores with no imposed symmetry. Their M−N distances average 1.886(3) (**1**), 2.104 (**2**), and 2.21(1) Å (**3**), which lie within the range of M−N single bonds reported for these elements;[4] cf. 1.849 Å in {Ge(μ-NMes*)}2,[13] 1.875 Å in Ge{N(SiMe3)2}2,[29] 2.03 Å (avg) in Sn{N(H)Mes*}2,[13,21] 2.09 Å in Sn{N(SiMe3)2}2,[29] 2.23 Å (avg) in Sn{μ-(NC6H3-2,6-Pri2)}4,[27] and 2.24 Å in Pb{N(SiMe3)2}2.[29] The internal ring angles at the metals average 81.2(2)° (**1**), 77.62(5)° (**2**), and 76.9(1)° (**3**), and those at the nitrogen are 99.25(14)° (**1**), 98.71(16)° (**2**), and 99.00(10)° (**3**). The distances between the centroids of the flanking mesityl rings and the group 14 elements (shown as dashed lines in Figure 2) are all longer than 3.1 Å and indicate probable weak dipolar interactions. The nitrogen atoms have planar coordination, which is typical for amido groups bound to heavier group 14 elements[4] but the M_2N_2 rings are characterized by significant folding (Figure 2) along the M---M axis. For the germanium compound **1**, however, the folding is relatively small, with a dihedral angle of 172.4° between the two NM_2 planes. This is in contrast to the essentially planar cores in the less hindered dimeric {Ge(μ-NMes*)}2[13] and trimeric {Ge(μ-NC6H3-2,6-Pri2)}3.[7,14] For **2** and **3**, the folding is significantly greater at 148.3° and is almost equal for both the tin (**2**) and lead (**3**) derivatives (Figure 2). This folding trend correlates with that seen for the X---M---X (X = centroid of Mes groups) angles, which are ca. 130° for **1**, ca. 102° for **2**, and ca. 103° for **3** (Table 2). This unprecedented folding, with syn disposition of the aryl substituents relative to the imidometal core, seems likely to be due to the weak flanking aryl---M attraction not possible in the planar rings stabilized by Mes*[13] or C6H3-2,6-Pri2 groups[7,13] and is probably increased by the larger size of tin and lead atoms.

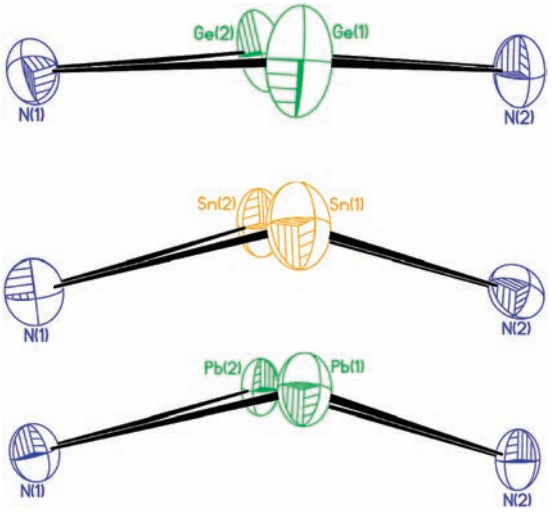

Figure 2. Views of the M_2N_2 cores in **1**−**3** (top to bottom) along their M---M axes, illustrating the ca. 7° (**1**) and ca. 31° (**2** and **3**) folds away from coplanar.

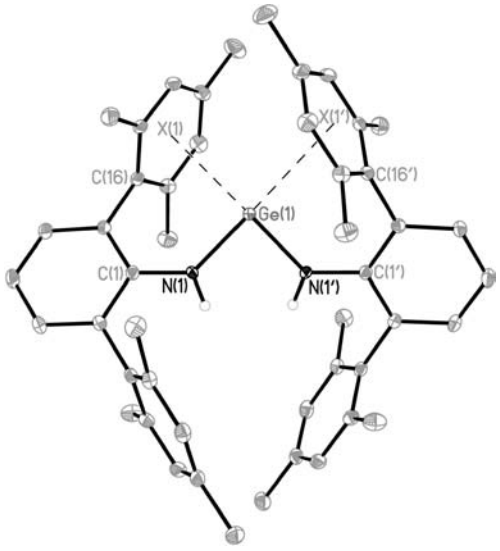

Figure 3. Thermal ellipsoid (30%) drawing of **4**. Hydrogen atoms (except N−H) and disordered component atoms are not shown. Ge(1)−N(1)−N(1)′ 1.896(2) Å; N(1)−Ge(1)−N(1)′ 88.44°; Ge(1)---X(1)−X(1)′ 3.106(2) Å; X(1)---Ge(1)---X(1)′ 102.1° . Symmetry transformations used to generate equivalent atoms (′): $-x+1, y, -z+{}^1/_2$.

The structures of **4**−**6** are shown in Figures 3−5, and selected structural data are given in Table 3. The compounds are monomers with V-shaped MN_2 coordination. The N(H)−M−N(H) angles are each less than 90° and have the values 88.6(2)° (**4**), 87.07(8)° (**5**), and 87.47(9)° (**6**.) An acute interligand angle is rare for germanium, tin, or lead two-coordinate derivatives of monodentate alkyl, silyl, or amido ligands, with the only example being the 89.6(6)° N−Sn−N angle in Sn{N(H)Mes*}2 (the standard deviation is large enough to encompass a 90° bending angle, however).[13,21] In contrast, several two-coordinate

(29) Fjeldberg, T.; Hope, H.; Lappert, M. F.; Power, P. P.; Thorne, A. J. *J. Chem. Soc., Chem. Commun.* **1983**, 639.

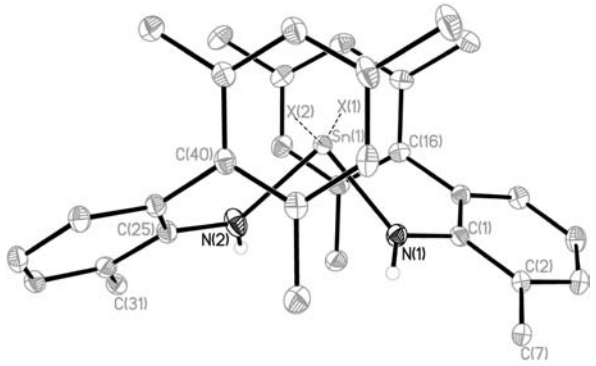

Figure 4. Thermal ellipsoid (30%) drawing of **5**, illustrating the coordination of the tin atom by the nitrogen atoms and centroids X(1) and X(2) of two flanking mesityl groups. Hydrogen atoms (except N−H) are not shown, and the positions of the two noninteracting flanking Mes groups (lower) are indicated only by their ipso C(7) and C(31) atoms. Sn(1)−N(1) 2.096 Å; Sn(1)−N(2) 2.103 Å; Sn(1)---X(1) 3.039 Å; Sn(1)---X(2) 2.976 Å; N(1)−Sn(1)−N(2) 87.1°; X(1)---Sn(1)---X(2) 160.0°.

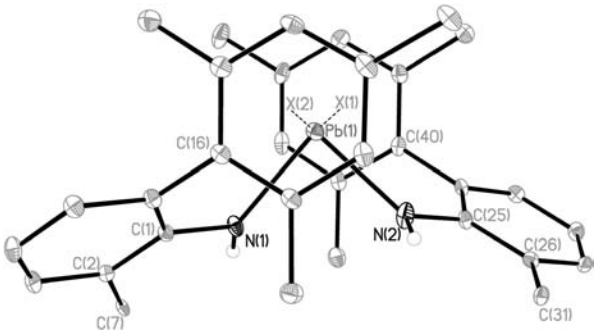

Figure 5. Thermal ellipsoid (30%) drawing of **6**, illustrating the coordination of the lead atom by the nitrogen atoms and centroids X(1) and X(2) of two flanking arenes. Hydrogen atoms (except N−H) are not shown, and the positions of the two noninteracting flanking arenes (lower) are indicated only by their ipso C(7) and C(31) atoms. Pb(1)−N(1) 2.193 Å; Pb(1)−N(2) 2.205 Å; Pb(1)---X(1) 2.989 Å; Pb(1)---X(2) 2.943 Å; N(1)−Pb(1)−N(2) 87.5°; X(1)---Pb(1)---X(2) 164.9°.

alkoxo and aryloxo group 14 element derivatives with acute interligand angles at M have been reported.[30−34] Seemingly, for these more electronegative ligands, the electron density in the bond is concentrated close to the coordinating ligand atom (i.e., oxygen), thereby reducing the repulsion between the metal−ligand bonding pairs. By the same token, the lone pair on metal(II) expands, which causes closure of the interligand angle below 90° as a result of electrostatic repulsion. For derivatives of primary amido ligands, angular closure below 90° is possible because of the small size of the hydrogen substituent. Compound **4** is unique in this series in that N(H)Ar$^{\#}$ substituents are approximately syn with respect to the GeN_2 plane, whereas **5** and **6** demonstrate an anti configuration of the N−H

Table 3. Selected Distances (Å) and Angles (deg) for Compounds **4**−**6**[a]

	$Ge\{H(N)Ar^{\#}\}_2$ (**4**)	$Sn\{H(N)Ar^{\#}\}_2$ (**5**)	$Pb\{H(N)Ar^{\#}\}_2$ (**6**)
M−N	1.896(2)	2.103(2)	2.205(2)
		2.096(2)	2.193(2)
N−C	1.384(3)	1.380(3)	1.375(3)
		1.381(3)	1.367(3)
M---X	3.106(2)	3.039(2)	2.989(2)
		2.976(2)	2.943(2)
N−M−N	88.6(2)	87.07(8)	87.47(9)
X---M---X	102.1(2)	160.0(2)	164.9(2)
dihedral N−M−N/X---M---X	47.9(3)	82.4(2)	83.6(2)

[a] X refers to the centroid of the flanking aryl ring. A prime denotes atoms generated by the two-fold symmetry ($1 - x$) operation for the M = Ge compound **4**.

bonds. The structures of **4**−**6** may be contrasted with the bridged dimeric structure of the unstable primary amide $Sn_2\{N(H)C_6H_3\text{-}2,6\text{-}Pr^i{}_2\}_4$;[27] **4** is characterized by a 2-fold axis of rotation that bisects the N(1)−Ge(1)−N(1A) bond angle, whereas the structures of **5** and **6** have no crystallographically required symmetry. The M−N bond lengths are 1.896(2) (**4**), 2.103(2) (**5**), and 2.205(2) Å (**6**), which are similar to those observed in **1**−**3**. Compounds **4**−**6** also exhibit M---X interactions to centroids of two of the flanking mesityl rings, ranging from 2.943(2) (**6**) to 3.106(2) Å (**4**). These distances are shorter than those in **1**−**3** and decrease as the group is descended, indicating that the metal−ring dipolar interactions increase in strength with increasing atomic number, possibly as a result of the increasing electropositive character of the metals. The stronger dipolar (δ^-)aryl---(δ^+)M interactions, combined with the larger sizes of tin and lead (1.41 and 1.45 Å),[16] result in a closer approach of the flanking rings to the metal, and a wider angle between the two M---X vectors results. The larger sizes of the tin and lead atoms also permit these interactions to occur on either side of the MN_2 plane such that the resulting X---M---X angles are 164.9(2)° (**6**) and 160.0(2)° (**5**), whereas the smaller size of germanium imposes a much narrower angle of 95.0(2)° in **4** (Figures 3−5). The dihedral angles between the X---M---X and N−M−N planes, 83.6(2)° (**6**), 82.4(2)° (**5**), and 47.9(3)° (**3**), show a similar trend (Table 3). These angular differences also suggest a greater tendency for π-electron density on the flanking arenes to interact with the empty p orbital on metal(II) for the heavier, more electropositive members of the group (Sn or Pb). Aryl---M interactions have been seen in a variety of other terphenyl-supported low-coordinate metal or metal−metal-bonded complexes and most frequently in low-coordinate transition-metal derivatives.[35,36]

Electronic Spectra. The large size of the Ar$^{\#}$ substituent stabilizes the two-coordinate, V-shaped geometries at the metal atom(s) in compounds **1**−**6**. UV−visible spectra reveal metal lone pair to empty p orbital (n → p) transitions typical for monomeric amidogermylenes, -stannylenes, and -plumbylenes, respectively.[4] The energy of this HOMO → LUMO transition decreases in the sequence

(30) Çetinkaya, B.; Gumrukcu, I.; Lappert, M. F.; Atwood, J. L.; Rogers, R. D.; Zaworotko, M. J. *J. Am. Chem. Soc.* **1980**, *102*, 2088.
(31) Fjeldberg, T.; Hitchcock, P. B.; Lappert, M. F.; Smith, S. J.; Thorne, A. J. *J. Chem. Soc., Chem. Commun.* **1985**, 923.
(32) Weinert, C. S.; Fanwick, P. E.; Rothwell, I. P. *Dalton Trans.* **2002**, 2948.
(33) Dickie, D. A.; MacIntosh, I. S.; Ino, D. A.; Hi, Q.; Labeodan, O. A.; Jennings, M. C.; Schatte, G.; Walsby, C. J.; Clyburne, J. A. C. *Can. J. Chem.* **2008**, 20.
(34) Barnhart, D. M.; Clark, D. L.; Watkin, J. G. *Acta Crystallogr.* **1994**, *C50*, 702.
(35) Nguyen, T.; Panda, A.; Olmstead, M. M.; Richards, A. F.; Stender, M.; Brynda, M.; Power, P. P. *J. Am. Chem. Soc.* **2005**, *127*, 8545.
(36) Merrill, W. A.; Brynda, M.; Yeagle, G. J.; Stich, T. A.; De Hont, R.; Fettinger, J. C.; Reiff, W. M.; Schulz, C. E.; Britt, R. D.; Power, P. P. *J. Am. Chem. Soc.* **2009**, *131*, 12693–12702.

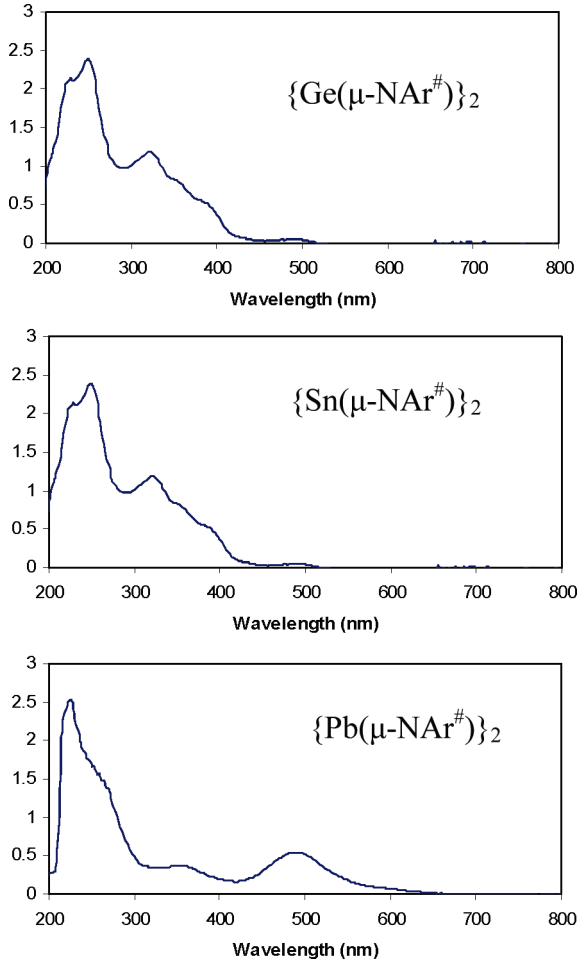

Figure 6. Electronic absorption spectra of ca. 0.1 mM hexane solutions of **1**−**3**.

Ge > Sn > Pb for both the imido series **1**−**3** (Figure 6) and the amides **4**−**6**. However, the imido derivatives are more intensely colored, and their spectra are more complex than those of the amido counterparts. For example, the molar absorptivity ε calculated for the principal absorption observed for the deep-red imidotin compound **2** (λ = 410 nm) is around 7800 M^{-1} cm^{-1}, whereas the analogous absorption seen in the bisamidotin **5** (λ = 420 nm) gives an ε value of 5000 M^{-1} cm^{-1}. A more dramatic difference is observed in the electronic spectra of the deep-purple imide **3** (λ = 490 nm, ε = 14 700 M^{-1} cm^{-1}) and the pale-yellow amide **6** (λ = 448 nm, ε = 3800 M^{-1} cm^{-1}). The less intense absorptions in **5** and **6** in comparison to **2** and **3** may also be due to the partial quenching of the n → p transition by the stronger metal---arene interactions. As shown in Figure 6, the centroids of the flanking arenes interact with M above and below the N−M−N plane and thus interact directly with the valence 5p or 6p orbitals involved in the n → p transition.

The pair of germanium compounds **1** and **4** displays a different intensity pattern from their tin and lead counterparts. The intensely red-colored imide **1** features a maximum at 322 nm (ε = 9500 M^{-1} cm^{-1}), with less intense shoulder absorptions at 356 and 388 nm. The yellow amide **4** shows an almost 50% greater ε value of 13 750 M^{-1} cm^{-1} for its transition at 380 nm. It is worth noting that the Ge---flanking ring interactions in **4** are not oriented directly above and below the MN_2 coordination plane (dihedral N−M−N/X---M---X angle 47.9(3)°, canted ca. 45° from perpendicular) unlike in **5** and **6** (canted ca. 15−20° from perpendicular; Table 2) and so do not strongly interact with the Ge 4p orbital. This is also refelected in the longer M---X distances in **4** in comparison to those in **5** and **6**. Thus, the n → p transition in **4** may not be quenched to the same extent as the corresponding transitions in **5** and **6**.

Heteronuclear NMR Spectroscopy. The ^{119}Sn NMR spectrum of **2** displays a downfield signal at δ 738.9, which is consistent with its formulation as a two-coordinate monomer.[22,37] The shift is similar to 776 ppm found for the well-known monomeric tin(II) amide starting material $Sn\{N(SiMe_3)_2\}_2$.[38] The chemical shifts are over 400 ppm downfield of the δ 315 signal reported for the tetrameric $\{Sn(\mu\text{-}NC_6H_3\text{-}2,6\text{-}Pr^i_2)\}_4$.[27] The latter species features three-coordinate tin atoms, which causes the upfield shift relative to **2**. However, the shifts of the tetramers are quite sensitive to the nitrogen substituents so that chemical shifts in the range 742−797 ppm have been observed for $\{Sn(NSiBu^tMe_2)\}_4$[39] and $\{Sn(NEMe_3)\}_4$ (E = Si,[40] Ge,[41] or Sn[41]). In contrast to these data, the 118.9 ppm shift found for the bisamide **4** is ca. 620 ppm downfield of that for **2**. This suggests a more shielded environment for the tin nucleus and is consistent with the ca. 0.13 Å closer aryl---Sn approaches (Figure 4 and Table 2) such that the tin may be regarded as quasi-four-coordinate with consequent greater electronic shielding. The ^{207}Pb NMR signals found for the lead derivatives **3** and **6** also appear in a region typical for divalent amides of that metal[42] and displayed a trend similar to that of their tin counterparts, with chemical shifts of +5019 (**3**) and +2871 (**6**) ppm, respectively. Like its tin counterpart **4**, the chemical shift of **6** lies well upfield of that of **3** most likely because of the greater shielding at the metal by the flanking aryl rings, where the closest aryl---Pb distance in **6** (2.943 Å; Figure 5) is ca. 0.15 Å shorter than that in the amide **3** (3.115 Å). The chemical shift observed for **4** is similar to the +2956 ppm reported for the dimeric compound $[\overline{Pb\{N(Pr^i)(SiMe_2)_2N(Pr^i)\}}]_2$,[43] which probably dissociates in solution to monomers featuring two-coordinate lead. No chemical shifts for imidolead dimers have been reported, but the +5019 ppm found for **3** is close to those observed for monomeric amides of lead.[42] For example, a signal at +4916 ppm was found for the monomeric $Pb\{N(SiMe_3)_2\}_2$ starting material used in this work, and a signal at +4900 ppm was observed for $[\overline{Pb\{N(Bu^t)(SiMe_2)_2N(Bu^t)\}}]_2$.[44] It seems clear that both the tin and lead NMR chemical shifts are very sensitive to relatively weak metal−ligand interactions, and the significant structural differences (especially the different secondary metal−ligand

(37) Wrackmeyer, B. *Annu. Rep. NMR Spectrosc.* **1999**, *38*, 203.
(38) Wrackmeyer, B. *J. Magn. Reson.* **1985**, *61*, 536.
(39) Veith, M.; Opsölder, M.; Zimmer, M.; Huch, V. *Eur. J. Inorg. Chem.* **2000**, 1143.
(40) Eichler, J. F.; Just, O.; Rees, W. S. *Phophorus, Sulfur, Silicon Relat. Elem.* **2004**, *179*, 715.
(41) Eichler, J. F.; Just, O.; Rees, W. S. *Inorg. Chem.* **2006**, *45*, 6700.
(42) Wrackmeyer, B. *Annu. Rep. NMR Spectrosc.* **2002**, *47*, 1.
(43) Wrackmeyer, B.; Stader, C.; Horchler, K.; Zhou, H. *Inorg. Chim. Acta* **1990**, *176*, 205.
(44) Wrackmeyer, B.; Horchler, K.; Stader, C. *J. Magn. Reson.* **1989**, *83*, 601.

interactions) between the dimeric imido compounds **1**−**3** and their monomeric amido counterparts **4**−**6** are strongly manifested in their ^{119}Sn and ^{207}Pb NMR experiments, as well as in their UV−visible spectra.

Conclusions

The imido compounds **1**−**3** comprise the first homologous series of dimeric heavier group 14 element imides. They display a folded M_2N_2 core not seen in the previously reported planar $\{Ge(\mu\text{-}NAr)\}_2$ structures.[13,15] The monomeric amides **4**−**6** also represent an isoleptic series of heavier group 14 element nitrogen derivatives. Like the series **1**−**3**, they display notable structural and spectroscopic trends that vary as the group is descended, in large part because of an increasing attraction (Ge < Sn < Pb) of the flanking aryl π-electron density on the ligands to the metal. The electron-rich flanking aryl rings on the ligands are drawn closer to the coordinatively unsaturated metal atoms in these compounds in the order Ge < Sn < Pb, and these interactions have a major effect on their spectral properties.

Acknowledgment. We thank the National Science Foundation (Grant CHE-0948417) for financial support.

Supporting Information Available: Crystallographic information files (CIFs) for **1**−**6**. This material is available free of charge via the Internet at http://pubs.acs.org.